



DOI: 10.34910/MCE.104.1

Failure mechanism and slope factors for a footing resting on slopes

R.P. Shukla^{a*}, R.S. Jakka^b

^a Department of Civil Engineering, National Institute of Technology Srinagar, Srinagar, India

^b Department of Earthquake Engineering, IIT Roorkee, Roorkee, India

*E-mail: rpshukla.2013@iitkalumni.org

Keywords: slope, footing, setback, bearing capacity, slope factor, failure mechanism

Abstract. The behaviour of a footing affected significantly with the presence of the slope. The effect of slope on the bearing capacity, slope factor, and failure mechanism has been explored using limit analysis. Both lower and upper bound bearing capacities are determined, and average values are reported. The bearing capacity increases with an increase in the setback, footing depth, and angle of internal friction of soil, but reduces with an increase in slope angle. However, the slope factor decreases with an increase in footing depth, slope angle, and angle of internal friction of soil, but increases with the setback. The failure mechanism as well slope factors change substantially with an increase in the angle of internal friction of soil and slope angle. The failure mechanism of the foundation changes from bearing capacity to combined mode with an increase in the slope. The results of small-scale model testing are compared with numerical study results. Finally, nonlinear regression equations are developed to predict bearing capacity factor, slope factor, and the critical setback for a footing resting on a slope.

1. Introduction

Footings are most often built on the slopes under various circumstances. The footing is subjected to less confining pressure on the sloping side, and soil tends to move toward the slope. It makes the behaviour of footing dissimilar to those resting on the level ground. The bearing capacity on a slope is either less than or equal to the footing resting on the level ground [1]. Footings resting precisely on the slope crest possess the minimum bearing capacity, which improves with an increase in the setback (B') between the footing and slope crest.

A number of studies have analysed the footing resting on the slopes under various loading conditions. Many of the available studies are an extension of bearing capacity methods for level ground. There are two cases possible: (i) footing either resting on a slope or resting precisely on slope crest; (ii) the footing resting adjacent to the slopes with some setback. Most of the studies have considered the case first [2–13]. Some studies have also analysed the footing resting adjacent to the slope crest with some setback [14–29]. Most of the studies were mainly focused on determining the bearing capacity without considering the mechanism of failure and slope factor. Few studies presented the slope factor, which indicates the effects of slope on the bearing capacity. The bearing capacity of footing resting on the slopes can be determined directly by means of slope factor if the bearing capacity for the level ground is known.

The earlier presented slope factors are mostly valid for the footings, resting precisely on the slope crest. The given slope factors are primarily applicable to surface footings. Further, there are discrepancies in the effect of the internal friction angle on the slope factor. Some studies observed the slope factor to be independent of the angle of internal friction [2, 3, 26]. Other studies observed the reduction in slope factor with an increase in the angle of internal friction of soil [1, 15, 19, 24, 28]. However, Castelli and Motta [29] made the contrary observation. Similarly, Shukla and Jakka [18] also observed an increase in the slope factor with an increase in the undrained shear strength of purely cohesive soil. It is also observed that the bearing capacity factors are varying significantly from study to study. The variations are sometimes even up to 100 %. It creates confusion for practicing engineers to decide upon the appropriate bearing capacity

Shukla, R.P., Jakka, R.S. Failure mechanism and slope factors for a footing resting on slopes. Magazine of Civil Engineering. 2021. 104(4). Article No. 10401. DOI: 10.34910/MCE.104.1



This work is licensed under a [CC BY-NC 4.0](https://creativecommons.org/licenses/by-nc/4.0/)

factor. Most of the earlier studies used the limit equilibrium method to determine bearing capacity, which significantly underestimates the bearing capacity. A few studies have also used limit analysis but used either upper bound or lower bound. The present study considers the factors affecting slope factor and bearing capacity using the upper and lower bound limit analyses. The optimised value, which is an average of upper and lower bound, has been reported. Significant importance has been given to the failure mechanism. Few experimental studies have also been performed to support the numerical study results. Finally, predictive models were developed to predict the bearing capacity factor, slope factor, and critical setback.

2. Methods

The strip footing resting on a slope is analysed by considering full-scale numerical modelling and small-scale experimental modelling. Methodology for both methods has been discussed separately in the sections, namely, "2.1 Numerical modelling" and "2.2 Experimental modelling".

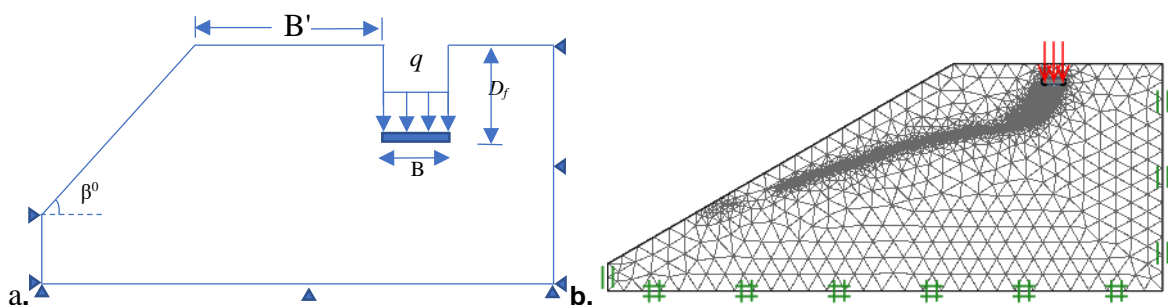
2.1. Numerical modelling

A 2D limit analysis finite element analysis was carried out to model the problem. A typical model considered in the study is shown in Fig. 1. The slope (β^0) has been assumed to be uniform throughout the soil slope. The footing width (B) has also been assumed constant throughout the study. Based on the slope geometry and setback, the domain area was selected large enough to reduce the boundary effect. The width and height of the domain were maintained $20 B$ and $10 B$, respectively. Increasing the number of elements to more than 5000 does not affect the results. Mesh was refined through adaptive iterations. Mostly, the results are stable after 3–4 iterations. A total of 7000 elements were used in the first iteration and increased to 10000 in the final iteration. The loading was applied in terms of load multiplier directly on the footing. The problem geometry and numerical modelling are shown in Fig. 1 (a, b).

The soil has been modelled as a drained material, and the Mohr-Coulomb model represents the shear strength. Both upper and lower bound analyses were performed using Optum G2 program to determine the ultimate capacity of footing. The average value has been adopted for further analysis. The detail of formulation for finite element upper bound and lower bound limit analysis is provided in earlier studies [30–33]. Makrodimopoulos and Martin [30] found that six nodes triangular elements are appropriate to determine the strict upper bound provided that sides are straight. Therefore, six node triangular elements have been used in the upper bound analysis to describe the soil elements. However, the lower bound analysis was performed with three-node elements. Second-order conic optimisation has been used to obtain the optimised value of the upper and lower bound loads. Makrodimopoulos and Martin [30–31] developed the formulation of yield criteria, equilibrium, and compatibility equations to second-order cone programming (SOCP). The poor optimisation may result in a low lower and a high upper bound. However, the application of SOCP enables to get the close upper and lower bound solution, which indicates the exact upper and lower bounds. The comparison of upper and lower bound bearing capacity is presented in section "3.1 Results and discussions".

2.2. Experimental modelling and procedure

In the experimental study, the strip footing of 1.15 m length and 0.09 m width has been tested in a tank with dimensions of 2 m \times 1.2 m \times 1.2 m. The model foundation testing setup is shown in Fig. 1 (c, d). Tank walls were marked with slope geometry to fill the sand in the desired slope. Rainfall technique, wherein sand is dropped from a fixed height, was used to pour the sand into the tank to attain the required density. Researchers had already used this technique to achieve reproducible densities [35]. Several trails were made to find the relation between the height of sand fall and the relative density of sand bed.



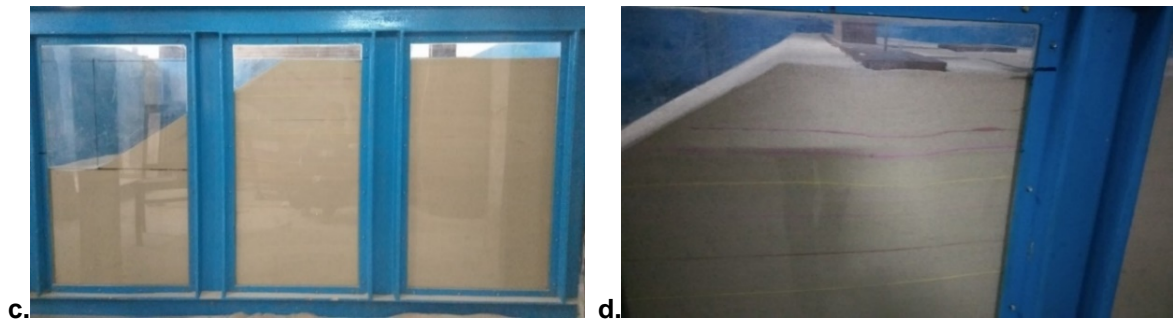


Figure 1. Model testing setup: (a) numerical model before iterations; (b) after three iterations; (c) experimental setup with prepared bed; (d) during loading stage.

Pulley and chain arrangement were used to maintain the required height of sand fall at regular intervals. After filling the tank up to the top level, the surface of the sand bed was levelled to maintain continuous contact between the soil and foundation. It also avoids the inclination of foundation. After this, the model foundation was placed on the top of the sand bed. This step requires high precision to maintain the level of the footing surface. The level of the model footing was checked using a spirit leveller to avoid any tilting. The footing was placed on the sand bed. The dial gauges were placed on the top of the footing to measure the settlement. The loading on the footing surface was applied using a mechanical arrangement. The load cell was connected to a transducer, which shows the magnitude of the applied load. The least count of the used load cell is 100 gms. Similar to plate load testing, load and settlement were measured for every load increment. The loading was applied in 10-15 load intervals. From the obtained load-settlement curves, the ultimate bearing capacity is determined.

2.3. Parameters considered in the analysis

The parameters studied in the present study include slope (β^0), setback (B'), angle of internal friction of soil (ϕ), and footing depth (D). The parameters range used in the study are presented in Table 1. The density of soil is varied based on the angle of shearing resistance of the soil. The unit weights used in the numerical study are 15, 17, and 19 kN/m³, and similarly, the stiffness of soil is assumed to be 10000 kN/m², 12500 kN/m² and 14000 kN/m², respectively. The setback and embedment depth are normalised with respect to the footing width (B).

Table 1. Parameters considered in the study.

ϕ (0)	B'/B	β (0)	D/B	No. of analysis
25	0, 1, 3, 5	0, 5, 10, 15, 20	0, 0.5, 1.0, 1.5, 2.0	600
30	0, 1, 3, 5	0, 5, 10, 15, 20, 25	0, 0.5, 1.0, 1.5, 2.0	720
35	0, 1, 3, 5, 7	0, 5, 10, 15, 20, 25, 30	0, 0.5, 1.0, 1.5, 2.0	1225
40	0, 1, 3, 5, 7, 9	0, 5, 10, 15, 20, 25, 30, 35	0, 0.5, 1.0, 1.5, 2.0	1680
45	0, 1, 3, 5, 7, 9	0, 5, 10, 15, 20, 25, 30, 35, 40	0, 0.5, 1.0, 1.5, 2.0	1890
Total number of the analysis				6115

For experimental model testing, cohesionless dry sand was used as a foundation bed. Many tests were conducted to determine the properties of the sand, such as sieve analysis, maximum dry density, minimum dry density, and specific gravity. Sieve analysis was performed as per IS: 2720-Part IV (1985) [36]. The description of soil properties and experimental testing program are shown in Table 2 and 3, respectively. The maximum and minimum sizes of sand particles are 1.18 mm and 0.1 mm, respectively.

Table 2. Description of soil.

Soil properties	Values	Soil properties	Values
Coefficient of Uniformity	1.60	Specific gravity	2.67
Coefficient of Curvature	1.00	Maximum density in gm/cm ³	1.67
Effective Size (D_{10}) mm	0.15	Minimum Density in gm/cm ³	1.43
D_{30} mm	0.19	Angle of internal friction of soil (ϕ^0)	37.50
D_{60} mm	0.24	Sand content	> 99 %

Table 3. Description of experimental testing on cohesionless soil slopes.

Relative density (%)	β^0	Setback (B'/B)	No. of tests
50 %	20, 25, 30	0, 1, 3, 6	12
60 %	20, 25, 30	0, 1, 3, 6	12
75 %	20, 25, 30	0, 1, 3, 6	12

3. Results and Discussions

3.1. Numerical study results

The effect of various factors on bearing capacity factor ($N_{\gamma q}$) and slope factor (S_f) is studied for a wide range of considered parameters. Both results are presented together for comparison purposes, as some trends are opposite for bearing capacity factor and slope factor. Error contributed to using the superposition method has been minimised by considering the effect of soil weight and the surcharge together through bearing capacity factor ($N_{\gamma q}$).

Fig. 2 shows the comparison of the upper and lower bound bearing capacity factors for different angles of internal friction of soil. The upper and lower bound bearing capacity factors are almost identical for soils with small internal friction angles (Fig. 2a). The difference between upper bound and lower bound increases with an increase in the angle of internal friction of soil; however, the error always remains trivial (< 3 %). The error is found to be small due to the application of second-order cone programming for optimisation. Therefore, it can be stated that the bearing capacity factors presented in the manuscript are mostly close to exact values.

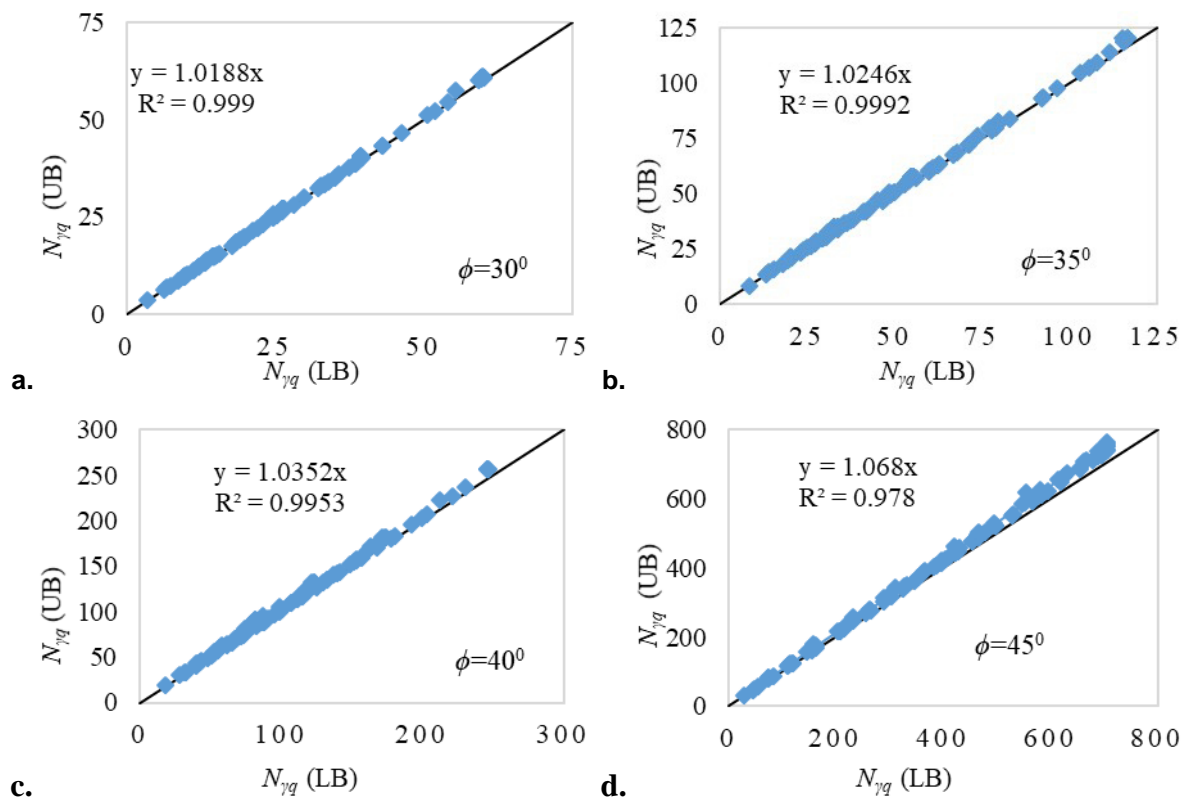


Figure 2. Comparison of upper and lower bounds bearing capacity factor for footing resting on slope: (a) $\phi = 30^\circ$; (b) $\phi = 35^\circ$; (c) $\phi = 40^\circ$; (d) $\phi = 45^\circ$.

Fig. 3 shows the typical variation in bearing capacity factor ($N_{\gamma q}$) and slope factor (S_f) with the setback for a soil with a friction angle of 35° . In all the cases, $N_{\gamma q}$ and S_f improve with an increase in the setback. The soil confinement increases, and the instability caused by the slope reduces with the setback. Also, passive resistance increases with an increase in setback due to an increase in a surcharge. The stiffness of the foundation-soil system enhances with an increase in the setback, which also improves the bearing capacity [12, 24]. These factors contribute to bearing capacity enhancement. The results are comparable to earlier studies of Rostami and Ghazavi [37] and Keskin and Laman [20] for an embedment depth of zero (Fig. 3 a, b). However, both the studies were confined to surface footings with a maximum setback of 5B.

The S_f is higher in the case of gentle slopes and becomes constant at a relatively small setback. The bearing capacity and slope factors become almost constant with a setback ratio (B'/B) of 3, 5, and 7 for foundation depth ratio (D/B) of 0, 0.5, and 1.0, respectively. The rate of increase in S_f and $N_{\gamma q}$ is large in steep slopes compared to gentle slopes. The curves are relatively gentle in case of footing with a higher depth ratio. It means the bearing capacity enhancement with a setback is relatively more in steep slope and footing resting on the ground surface.

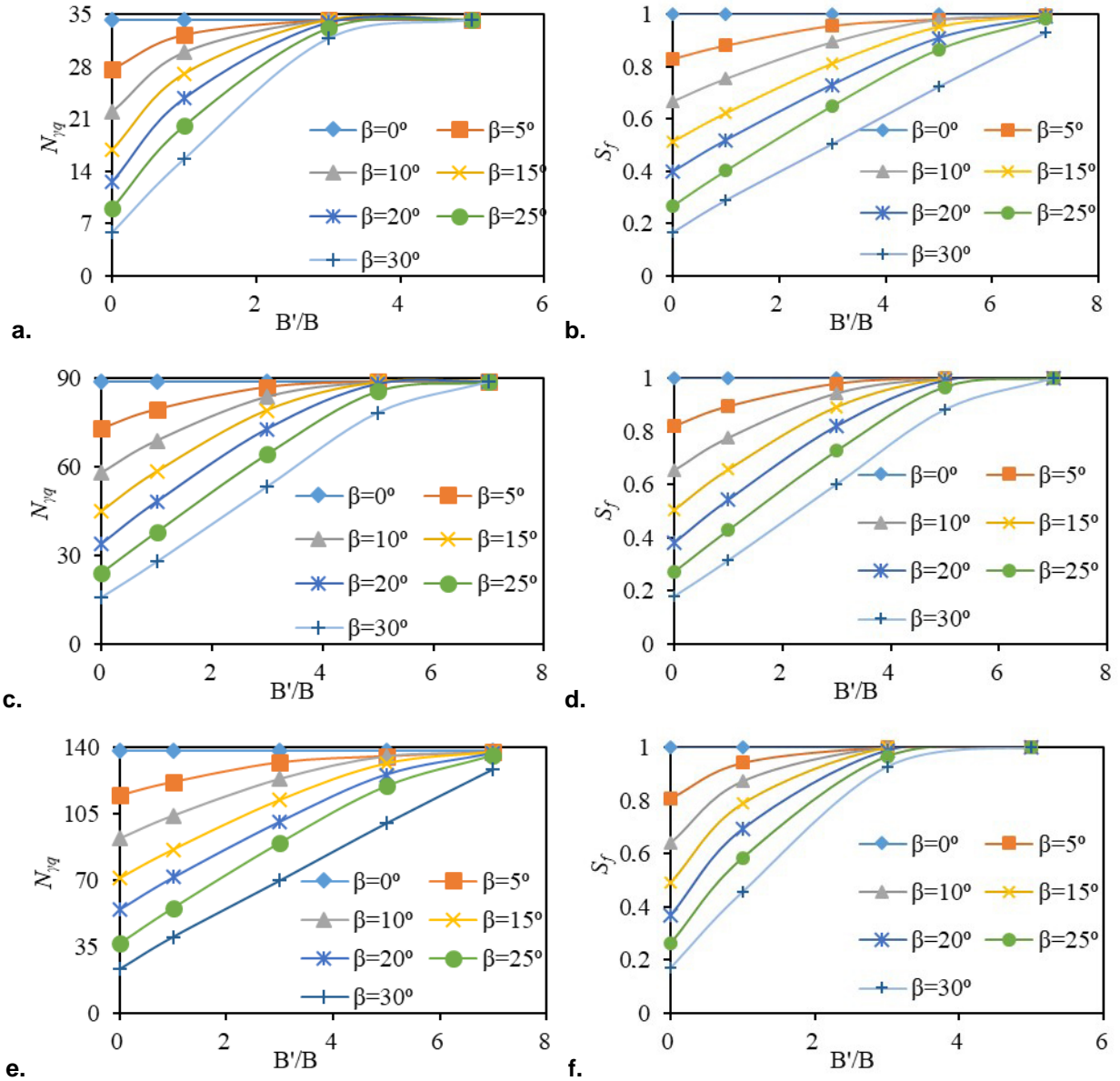


Figure 3. Effect of a setback (a) $N_{\gamma q}$, $D_f/B = 0$; (b) S_f , $D_f/B = 0$; (c) $N_{\gamma q}$, $D_f/B = 0.5$; (d) S_f , $D_f/B = 0.5$; (e) $N_{\gamma q}$, $D_f/B = 1.0$; (f) S_f , $D_f/B = 1.0$.

Fig. 4. shows that at a smaller setback, strength is mobilised only on the sloping side. It means that the soil on the sloping side entirely governs the behaviour of footing at a low setback. The strength mobilisation on the level side of the footing axis enhances with the setback. At a particular setback, strength mobilises equally on both sides of the footing axis, and the failure zone becomes almost symmetrical, and the slope factor also becomes close to one. This setback is stated as a critical setback. For the angle of internal friction of 35° , the slope influences the failure zone up to the setback of $7B-8B$. The influence of soil surcharge is absent at zero setbacks (Fig. 4a). The surcharge increases with an increase in the setback and reaches a maximum value at level ground. Therefore, bearing capacity increases with an increase in the setback. A similar observation was made in the experimental study carried by Chang *et al.* [38]. The slip surface direction changes from lateral to the upward direction with an increase in the setback (Fig. 4). The area within the failure zone or length of failure surface increases with an increase in the setback; therefore, bearing capacity increases also increases.

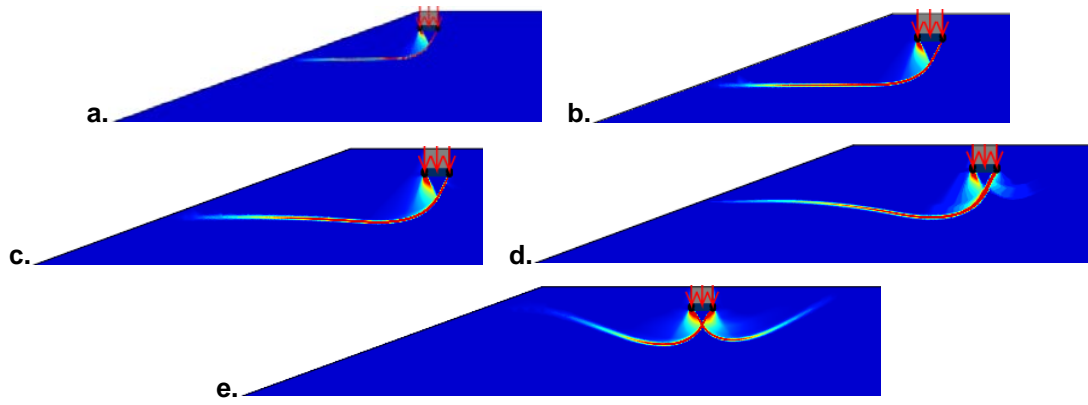


Figure 4. Failure mechanism for various setback for soil of internal friction 35°:
(a) $B'/B = 0$; (b) $B'/B = 1$; (c) $B'/B = 3$; (d) $B'/B = 5$; (e) $B'/B = 7$.

The typical variations in $N_{\gamma q}$ and S_f with the slope angle for soil with internal friction of 35° are shown in Fig. 5. The S_f as well $N_{\gamma q}$ reduces with an increase in slope, and the reduction depends on the embedment depth of foundation and setback. The reduction in $N_{\gamma q}$ and S_f with an increase in slope is very significant at zero setbacks. It is also observed that the reduction in bearing capacity factor, as well as slope factor, augments with an increase in the footing depth. In large setbacks, $N_{\gamma q}$ and S_f remain relatively unaffected with the change in slope.

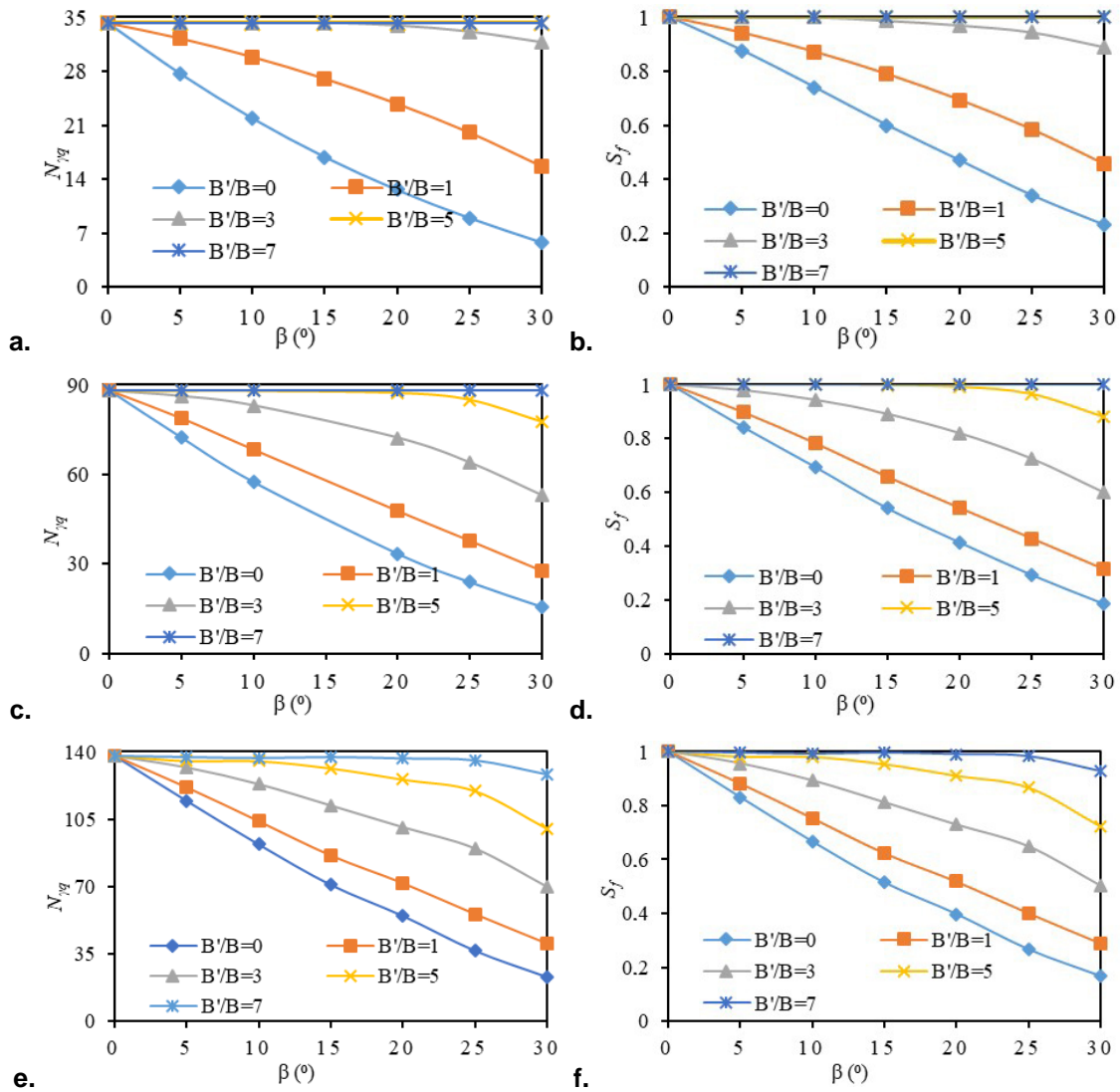


Figure 5. Effect of slope angle: (a) $N_{\gamma q}$, $D_f/B = 0$; (b) S_f , $D_f/B = 0$; (c) $N_{\gamma q}$, $D_f/B = 0.5$; (d) S_f , $D_f/B = 0.5$; (e) $N_{\gamma q}$, $D_f/B = 1.0$; (f) S_f , $D_f/B = 1.0$.

The effect of slope on the failure mechanism for a footing of depth ratio 1.0 is shown in Fig. 6. The results are shown for a footing resting at a setback of 5B on soil with internal friction of 35°. On level ground, the failure surface is symmetrical and gradually becomes one-sided with an increase in the slope (Fig. 6 a-d). It is due to a decrease in the shear dissipation on the level side of the footing. At steep slopes, the failure mode is a combination of the slope and bearing capacity failures (Fig. 6 d). Further increasing the slope results in an unstable slope. At this stage, the interaction of slope with the footing is maximum, and the failure is entirely a slope failure. This stage depends on the angle of internal friction of soil as well as loading intensity. The failure surface orientation is upward at a smaller slope (general shear failure) and is turning gradually toward the downward side, i.e., towards the slope base with an increase in the slope (Fig. 6 a-d).

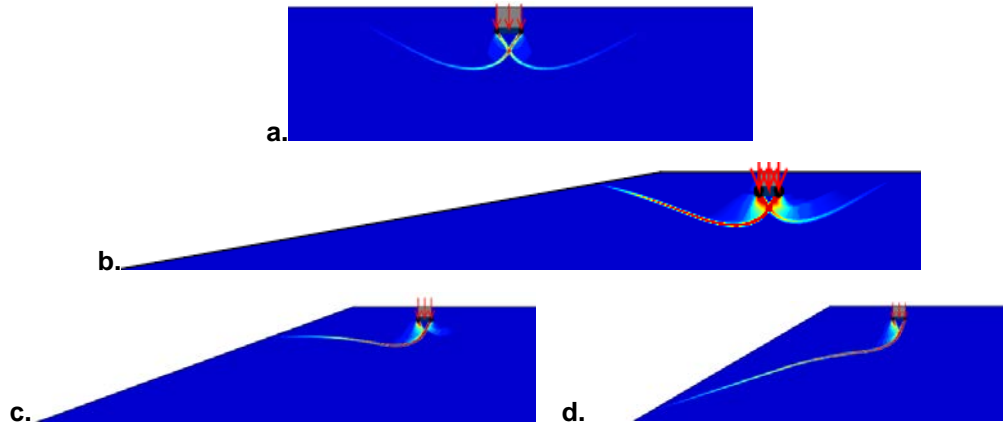
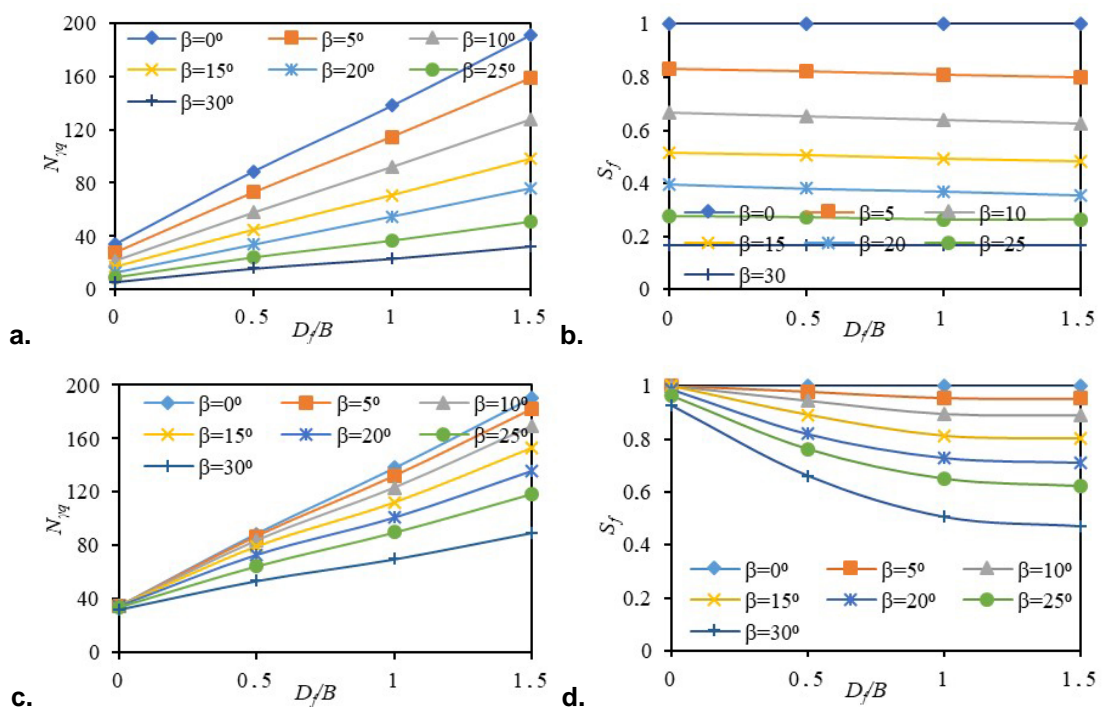


Figure 6. Failure mechanism for various slope gradients:
(a) $\beta = 0^\circ$; (b) $\beta = 10^\circ$; (c) $\beta = 20^\circ$; (d) $\beta = 30^\circ$.

Fig. 7 shows that $N_{\gamma q}$ increases and S_f decrease with an increase in embedment depth of footing. The contrary behaviour is observed as increasing the depth increases the bearing capacity relatively by a large amount on the level ground as compared to footings on slopes. The increase in footing depth indirectly increases the setback also (at the base level of footing). Therefore, the bearing capacity increases with the footing depth. The decrease in the slope factor indicates the increase in the adverse effect of the slope. The effect of footing depth is significant at a higher setback. The observation is contrary to Castelli and Motta [29], where the influence of embedment depth on S_f was found to be insignificant. The effect of depth ratio of footing is relatively more significant for soil with a low friction angle, and a similar observation has also been made for the footings resting on sloping ground. Garnier *et al.* [39] found the slope factor is always greater than 0.2 in steep slopes (3V: 2H) for soils with an internal friction angle of 40.5°. However, in the present study, it is found to be 0.14.



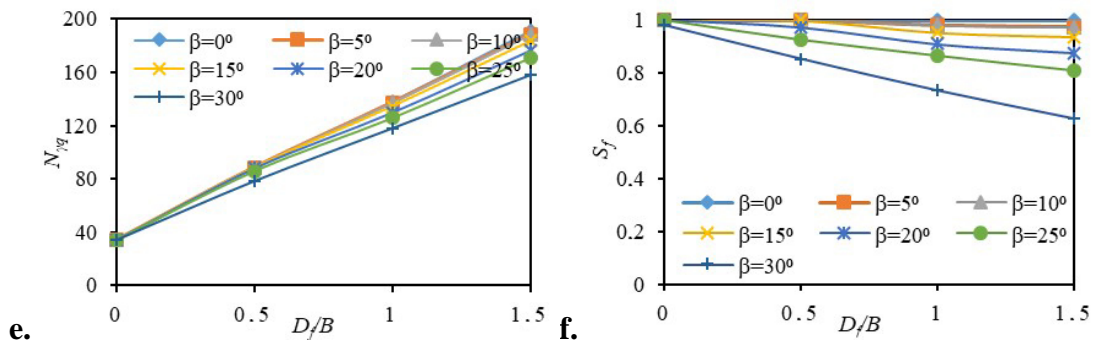


Figure 7. Effect of embedment depth of footing: (a) $N_{\gamma q}$, $B'/B = 0$; (b) S_f , $B'/B = 0$; (c) $N_{\gamma q}$, $B'/B = 3$; (d) S_f , $B'/B = 3$; (e) $N_{\gamma q}$, $B'/B = 5$; (f) S_f , $B'/B = 5$.

Fig. 8 shows that the failure surface is symmetrical about the footing axis, and is independent of the slope effect when a footing is resting on the ground surface. Therefore, the slope factor is either 1 or close to 1 (Fig. 8a). The footing resting on ground surfaces fails due to local shear failure (Fig. 10 a). An increase in the slip surface length and the area is observed with an increase in the footing depth, which increases the bearing capacity (Fig. 8 a, c, e). However, the contribution from the level side of the soil reduced with footing depth. It indicates the increased interaction between slope and footing, which decreases the slope factor. Initially, the failure surface orientation is upward (Fig. 8 a, b), but it changes from upward to lateral direction with an increase in footing depth (Fig. 8 b, c). Increasing the footing depth from 1B to 1.5B increases the failure zone area marginally (Fig. 8 c, d). Therefore, bearing capacity increases only slightly.

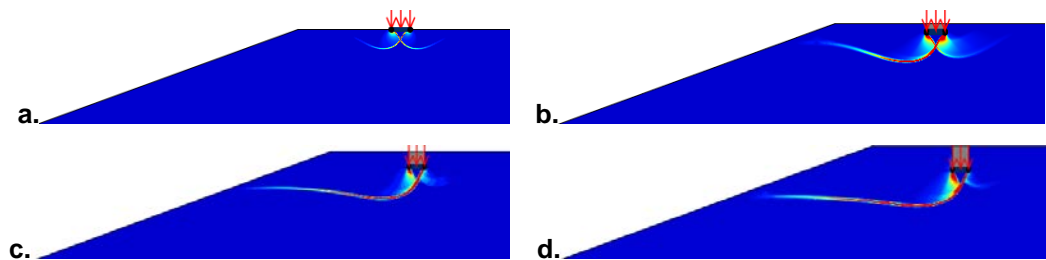
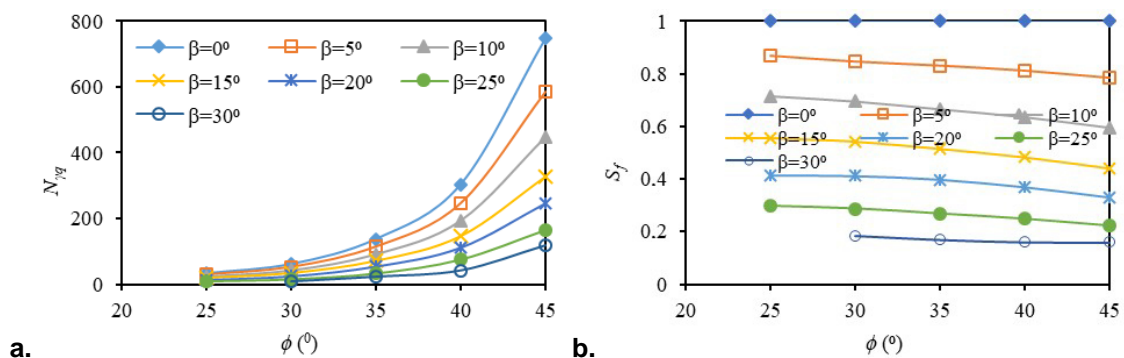


Figure 8. Effect of embedment depth of footing on failure surface: (a) $D_f/B = 0$; (b) $D_f/B = 0.5$; (c) $D_f/B = 1.0$; (d) $D_f/B = 1.5$.

3.1.4 Effect of angle of internal friction of soil

For a particular setback, slope, and embedment depth of footing, $N_{\gamma q}$ increases, and the S_f decreases with an increase in the angle of internal friction of soil (Fig. 9). The increase in $N_{\gamma q}$ with an angle of internal friction is relatively substantial in the level ground as compared to slopes. The reduction in S_f is relatively higher for a small setback and a steep slope. The soil with a higher angle of internal friction can be stable even at a higher inclination ($\beta = \phi^\circ$); therefore, the slope factor is relatively less. The relationship between S_f and friction angle of soil is linear for gentle slopes and becomes nonlinear with an increase in the slope. In soils with a higher internal friction angle, the pressure from the external load is dispersed over a relatively large area. Therefore, a large setback needs to be maintained to minimise the slope effects [22, 24]. Therefore, the slope factor reduces with an increase in the angle of internal friction of soil. This observation is contradictory to those made by Hansen [2], Vesic [3], Gemberlin [26], and Castelli and Motta [29].



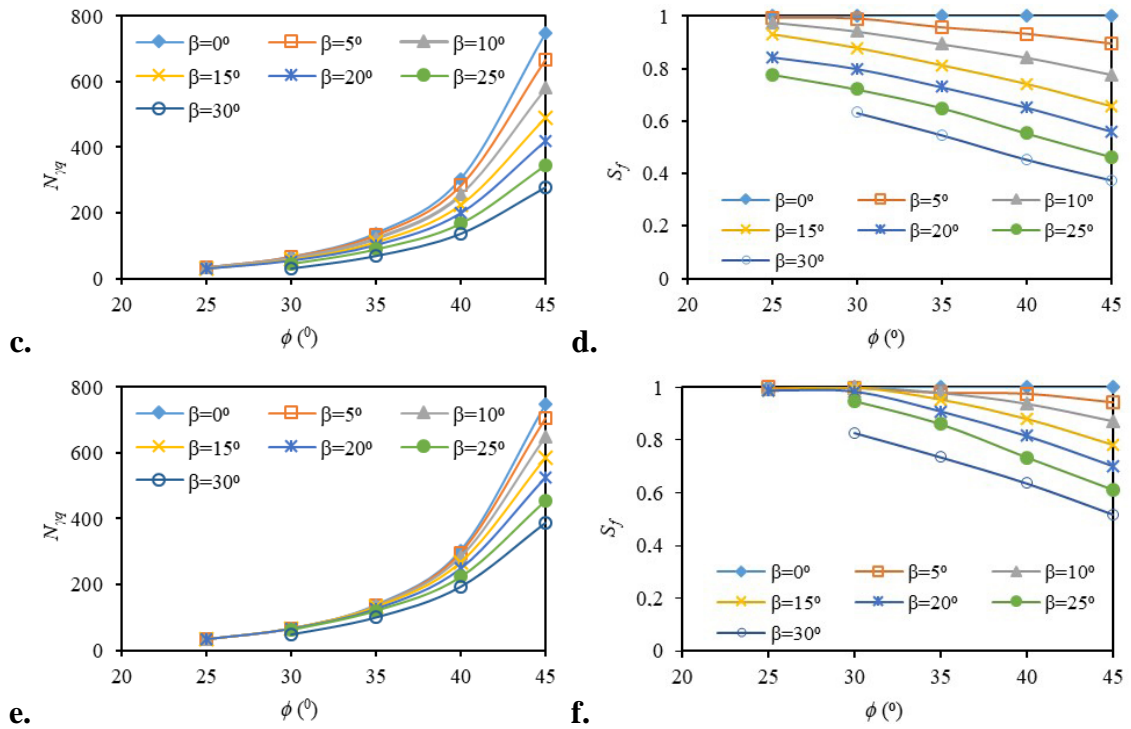


Figure 9. Effect of friction angle for a footing of zero embedment resting over soil of internal friction 35°: (a) $N_{\gamma q}$, $B'/B = 0$; (b) S_f , $B'/B = 0$; (c) $N_{\gamma q}$, $B'/B = 3$; (d) S_f , $B'/B = 3$; (e) $N_{\gamma q}$, $B'/B = 5$; (f) S_f , $B'/B = 5$.

The effect of the angle of internal friction of soil on the failure mechanism is shown in Fig. 10. An increase in the angle of internal friction of soil increases the failure zone area, which increases the bearing capacity (Fig. 10 a). Also, the failure is a local shear failure, and the slip surface is not developing clearly in soils with a low angle of internal friction (10 a). The slip surface/fracture surface is small and symmetrical about the footing axis for a soil with a small internal friction angle. Therefore, the slope factor is close to 1. The failure mechanism changes gradually from symmetrical to one-sided, increasing the soil angle of internal friction (Fig. 10 a-d). It indicates the effective transfer of stress (plastic zone) toward the slope-side due to early mobilization of strength. However, stresses are not mobilizing on the level side of the footing axis. Therefore, the slope factor reduces significantly.

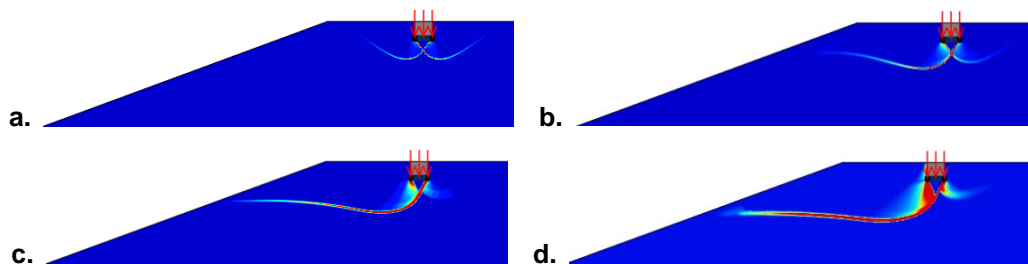


Figure 10. Effect of angle of internal friction of soil on failure mechanism: (a) $\phi = 25^\circ$; (b) $\phi = 30^\circ$; (c) $\phi = 35^\circ$; (d) $\phi = 40^\circ$.

Table 4. Slope factor for cohesionless soil slopes.

ϕ^0	β^0	S_f
25	05–20	0.5–1.0
30	5–20	0.45–1.0
	20–30	0.25–0.45
35	0–20	0.4–1.0
	20–30	0.20–0.4
40	0–20	0.35–1
	20–40	0.1–0.35
45	0–20	0.3–1
	20–45	0.05–0.30

3.2. Experimental study results and comparison

The load and settlement of footing were recorded for the various setback, slope, and relative density of soil. The load-settlement characteristic of footing resting on the slope is shown in Fig. 11. Failure points are clearly visible in almost all cases, which indicates general shear failure. General shear failures are observed in the numerical study as well. Fig. 11 (a, b) shows that the failure load increases with an increase in sand and setback density. The slope effect is shown in Fig. 11(c) for a footing resting at $B' = 0$ on soil with a relative density of 50%. It indicates that load-settlement behaviour changes significantly with the decrease in slope. The effect of slope on load-settlement characteristic is relatively more noticeable as compared to relative density and setback.

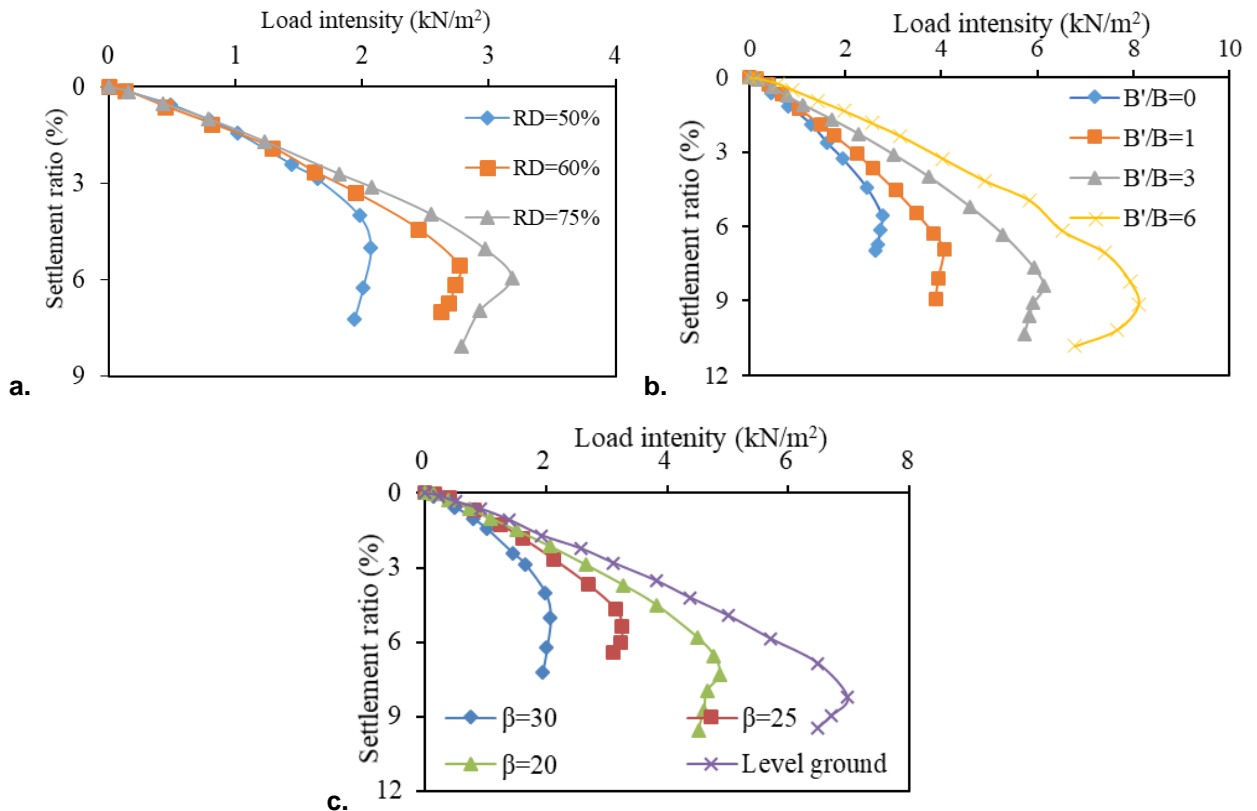


Figure 11. The load-settlement relationship for model footing: (a) effect of relative density; (b) effect of a setback; (c) effect of slope.

The results of the numerical study are compared with the experimental studies and shown in Fig. 12. The experimental and numerical study results are shown as dashed and continuous lines, respectively. The effect of the setback on S_f for a slope of 20° is compared in Fig. 12 (a). Similarly, the effect of the slope is compared in Fig. 12 (b). Though there is a small quantitative difference in the experimental and numerical study results, the qualitative similarity (result trends) exists between both cases. The rate of increase in S_f with the setback is more in the numerical study (Fig. 12 a). The difference is maximum for a small setback, which reduces with an increase in the setback. In soils with low friction angle (loose soils), the prevailing confining pressures and mobilised friction angles are almost identical in the experimental and numerical study. Therefore, the experimental results are reasonably close to the full-scale numerical study. The critical value of setback is also remained unaffected by the method of determination (experimental and numerical) for soils with a low angle of internal friction ($\phi < 35^\circ$). The difference in the results of full and small-scale testing may become noticeable with an increase in the angle of internal friction of soil. The small-scale model underestimates the severity of the slope effect compared to the full-scale study as prevailing confining pressure is higher in actual cases.

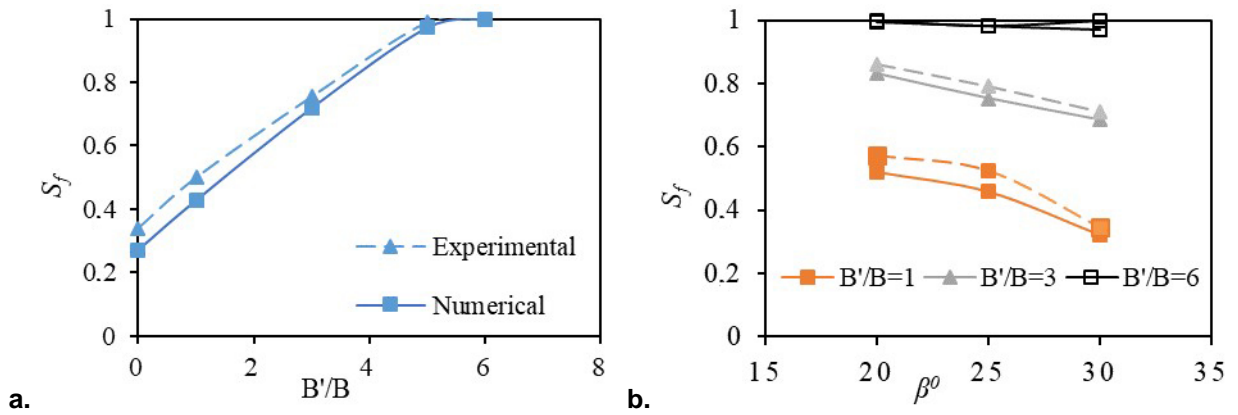


Figure 12. Comparison of experimental results with numerical results: (a) effect of a setback; (b) effect of slope.

Numerical results are also compared with earlier published results for a footing resting precisely on slope crest with zero setbacks and are shown in Fig. 13 [2, 14, 40–45]. It indicates that for the smaller angle of internal friction ($\phi = 20^\circ$), the values obtained through the present numerical study are almost of average values proposed by earlier studies (Fig. 13 a). However, for a higher angle of internal friction ($\phi = 40^\circ$), the values obtained through the present numerical study are either lower side or close to the average values proposed by earlier studies (Fig. 13 c).

In most of the cases, the bearing capacity factor is found close to Hansen's [2] and Giroud *et al.* [41]. This difference in the values is observed due to the different methodologies adopted by earlier studies. The reduction in bearing capacity with slope is significant in soil with a low internal friction angle ($\phi = 20^\circ$), which reduces with an increase in the internal friction angle ($\phi = 30^\circ, 40^\circ$). Bearing capacity is less than those presented by Chen and Davidson [43] using upper bound and is more than those given by Absi [40].

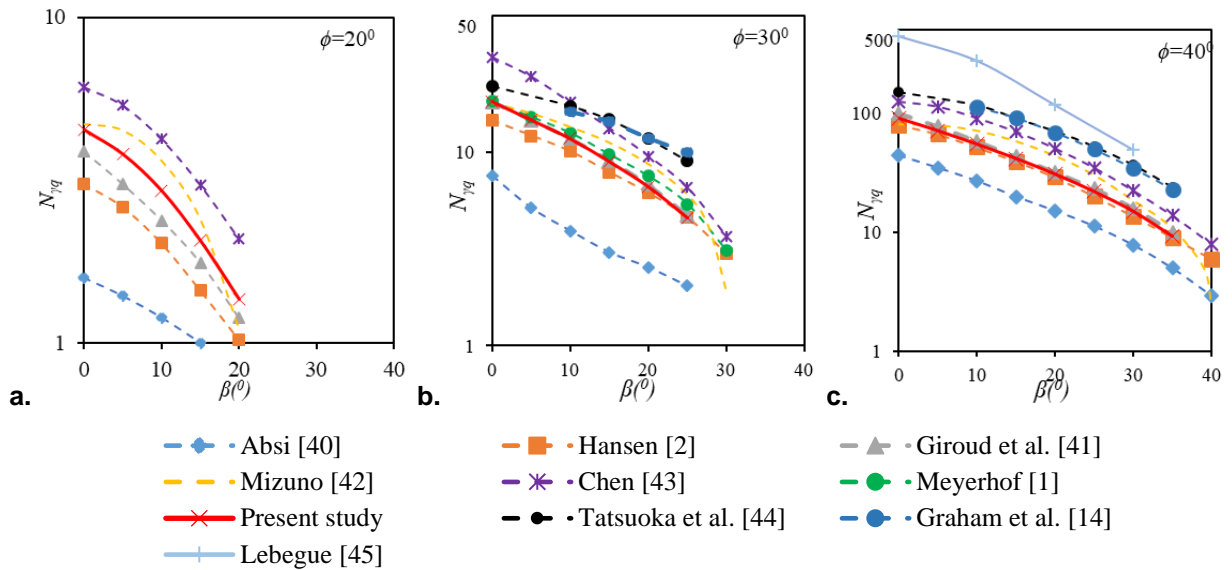


Figure 13. Comparison of results with earlier results for a footing resting precisely on slope crest: (a) $\phi = 20^\circ$, (b) $\phi = 30^\circ$, (c) $\phi = 40^\circ$.

3.3. Statistical analyses and validation of equations

Statistical analyses were also performed to develop nonlinear equations to predict bearing capacity, slope factor, and critical setback. It can be seen from the numerical analysis that setback, slope, soil friction angle, and footing depth influencing the bearing capacity of a footing on the slope. The numerical study results also show that the relationship between the independent parameters and S_f and $N_{\gamma q}$ is nonlinear. Consequently, nonlinearity needs to be considered while developing equations of S_f , $N_{\gamma q}$, and B' . The precise nonlinearity is not known initially. It is presumed that the S_f , $N_{\gamma q}$, and B' depend not only on four parameters but also on derivatives of these factors.

Initially, a total of 96 parameters, which are the function of initially known four independent variables, are considered in the regression analysis. Along with the multicollinearity, the R^2 was used to remove the

variables, not affecting bearing capacity. It is observed that only 12 parameters, including the four basic parameters, critically affect the slope factor. Later these 12 variables were used to develop the equation. Similarly, for developing the bearing capacity factor ($N_{\gamma q}$) equation, 14 variables and 9 variables have been used for the critical setback. Fig. 14 (a, b, c) compares observed and predicted slope factors and critical setback and bearing capacity factor.

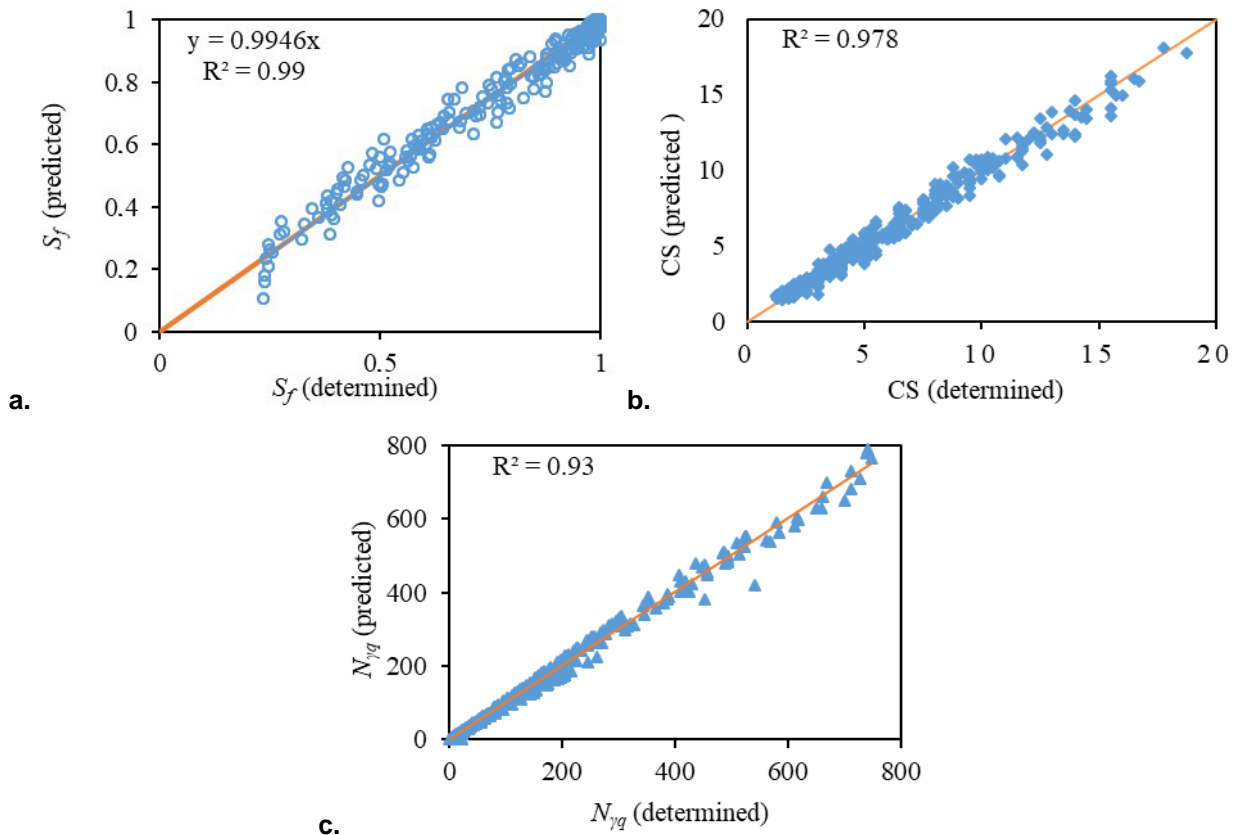


Figure 14. Determined vs. predicted values:

(a) slope factor; (b) critical setback; (c) bearing capacity factor ($N_{\gamma q}$).

$$S_f = 1 + 0.12(B'/B)(1 + 2.1 \tan \beta - 0.47 \tan \phi) - \tan \beta(1 - \tan \beta) - 0.04(D/B)(B'/B + 7.9 \tan \beta - D/B) - 0.015(B'/B)^2(1 - 0.33D/B - 0.66 \tan \phi) - 0.17 \tan \beta \tan \phi(B'/B + 5.3) \quad (1)$$

$$N_{\gamma q} = 400 - 100D/B(1 - \tan \phi) - 60B'/B \left[1 + 0.1(B'/B)^2 - 0.45(B'/B)\beta \right] - 27D/B(D/B - 0.5B'/B + 12(D/B)\beta) + 814(1 - 1.5 \tan \phi + 0.03\beta^2) - 1520 \tan \phi \left[1 - 0.9 \tan^2 \phi - 0.05(B'/B) \tan \phi \right] \quad (2)$$

$$CS = 2.5 - 1.2D/B \left[1 - 0.8(D/B) - 0.4 \tan \phi \right] - 5.5 \tan \phi(1 - \tan \phi - 3.2\beta) - 8.5\beta(1 - 1.3\beta - 0.6D/B) \quad (3)$$

$$N_{\gamma q(slope)} = N_{\gamma q(level\ ground)}(S_f) \quad (4)$$

$$\text{Bearing capacity on slope} = \text{Bearing capacity on level ground} * \text{Slope factor} \quad (5)$$

$$\text{Bearing capacity on slope} = \frac{1}{2} B \gamma N_{\gamma q(slope)} \quad (6)$$

where, S_f = Slope factor, B' = setback, B = width of footing, CS = critical setback, β = slope in degree, and ϕ = angle of internal friction of the soil in degree.

R^2 is reduced from 0.9925 to 0.9807 when the number of the insignificant variables were removed from the analysis. It confirms that the other dependents variables do not affect the bearing capacity, as assumed in the initial phase of the regression analysis. The slope factor (S_f), bearing capacity factor ($N_{\gamma q}$), and critical setback can be determined by Eqns. 1, 2, and 3, respectively. S_f cannot be more than 1, as bearing capacity on slopes may reach the maximum level ground. If equation 1 predicts values more than 1, then it should be corrected to 1. Eqn. 3 can be used to determine the critical location of the footing relative to the slope crest. Critical location means setback at which the effect of the slope is almost negligible. The slope factor can be also be used to assess the effect of slope angle on bearing capacity. Eqn. 4 is beneficial if the bearing capacity factor for the level ground is already known. Alternatively, bearing capacity can be determined by using Eqns. 5 and 6. These equations have developed considering the influence of the slope geometry, footing depth, setback, and the angle of internal friction of the soil.

A few earlier studies have given importance to setback and determined the critical setback, at which the effect of slope becomes negligible [17–18, 22, 24]. However, change in bearing capacity and slope factor is relatively more noticeable with a change in slope inclination and internal friction angle. Therefore, these factors need relatively more attention in design foundations. The foundation can be placed near to slope crest without much compromising bearing capacity if the slope is modified considering the steepness of slope and angle of internal friction of soil. The slope can be modified either by making it relatively gentle or enhancing the angle of internal friction of soil through various available techniques. Both options are feasible from a practical point of view. Therefore, it is suggested to place the footing close to the crest of the modified slope.

4. Conclusions

1. The presence of slope reduces the overall mobilisation of shear strength, particularly on the level side of the footing, which reduces the bearing capacity of footing. The range of slope factors varies from 0.05 to 1, depending on various factors. It indicates 95 % to 0 % reduction in bearing capacity of footing due to the adverse slope effects.
2. The bearing capacity factor increases and the slope factor reduces with an increase in the footing depth and angle of internal friction of soil due to change in failure mechanism.
3. The failure mechanism changes from both sides to one side with an increase in slope inclination, footing depth, and angle of internal friction of soil. Therefore, it is recommended to consider one side failure mechanism for designing the footings resting on slopes.
4. The effect of slope inclination and angle of internal friction of soil on bearing capacity, slope factor, and failure mechanism is relatively more noticeable than the footing depth and setback.
5. The increase in bearing capacity with setback contributes to an increase in strength mobilisation of soil and change in failure mechanism from local shear failure or rotational failure to general shear failure.
6. The load-settlement behaviour of footing improves with an increase in the setback and relative density of soil. However, the behaviour worsens with an increase in slope inclination. The model testing results are found reasonably close to numerical study.
7. Load-settlement plots and failure mechanisms show that the failure is bearing capacity rather than slope failure for the stable slopes. However, in the case of steep slopes or marginally stable slopes, the failure is a combination of slope and bearing failures.
8. The equation is also proposed to determine the critical location of footing relative to slope crest (critical setback). The proposed equations for slope factor, bearing capacity factor, and critical setback considers the possible factors affecting footing behaviour, such as footing depth, slope inclination, and soil strength parameter.
9. It is recommended to either modify the slope geometry or increase the soil strength and place the footing close to the slope crest.

References

1. Meyerhof, G.G. The Ultimate Bearing Capacity of Foundation on Slopes. 4th Int. Conf. on Soil Mech. and Foundation Engineering. 1957. 3. Pp. 384–386.
2. Hansen, J.B. A Revised and Extended Formula for Bearing Capacity. Dan. Geotech. Institute. 1970. Bulletin No. 28.

3. Vesic, A.S. Analysis of ultimate loads of shallow foundations. *Journal of the Soil Mechanics and Foundations Division*. 1973. 99(1). Pp. 45–73.
4. Bowles, J.E. (1988). *Foundation engineering and design*. McGraw-Hill, Inc.
5. Kumar, J., Mohan Rao, V.B.K. Seismic bearing capacity of foundations on slopes. *Geotechnique*. 2003. 53(3). Pp. 347–361.
6. Jahanandish, M., Keshavarz, A. Seismic bearing capacity of foundations on reinforced soil slopes. *Geotextiles and Geomembranes*. 2005. 23(1). Pp. 1–25.
7. Choudhury, D., Subba Rao, K.S. Seismic bearing capacity of shallow strip footings embedded in slope. *International Journal of Geomechanics*. 2006. 6(3). 176–184.
8. Kumar, J., Ghosh, P. Seismic bearing capacity for embedded footings on sloping ground. *Geotechnique*. 2006. 56(2). Pp. 133–140.
9. Huang, C.C., Kang, W.W. Seismic bearing capacity of a rigid footing adjacent to a cohesionless slope. *Soils and Foundations*. 2008. 48(5). Pp. 641–651.
10. Huang, C.C. Effects of horizontal and vertical seismic loads on the bearing capacity of a surface footing adjacent to a slope. *Soils and Foundations*. 2009. 49(2). Pp. 249–258.
11. Kumar, J., Chakraborty, D. Seismic bearing capacity of foundations on cohesionless slopes. *Journal of Geotechnical and Geo-Environmental Engineering*. 2013. 139(11). Pp. 1986–1993.
12. Varzaghani, I.M., Ghanbari, A. A new analytical model to determine dynamic displacement of foundations adjacent to slope. *Geomechanics and Geoenvironment*. 2014. 6(6). Pp. 561–575.
13. Chakraborty, D., Kumar, J. Seismic bearing capacity of shallow embedded foundations on a sloping ground surface. *International Journal of Geomechanics*. 2014. 15(1), 04014035.
14. Graham, J., Andrews, M., Shields, D.H. Stress characteristics for shallow footings in cohesionless slopes. *Canadian Geotechnical Journal*. 1988. 25(2). Pp. 238–249.
15. Saran, S., Sud, V.K., Handa, S.C. Bearing Capacity of Footings Adjacent to Slopes. *Journal of Geotechnical Engineering, ASCE*. 1989. 115(4). Pp. 553–573.
16. Lee, K.M., Manjunath, V.R. Experimental and numerical studies of geosynthetic-reinforced sand slopes loaded with a footing. *Canadian Geotechnical Journal*. 2000. 37(4). Pp. 828–842.
17. Huang, C.C., Kang, W.W. The effects of a setback on the bearing capacity of a surface footing near a slope. *Journal of Geo-Engineering*. 2008. 3(1). Pp. 25–32.
18. Shukla, R.P., Jakka, R.S. Determination and prediction of bearing capacity on clayey slopes. *Acta Geotechnica Slovenica*. 2019. 16(2). Pp. 50–65.
19. Krabbenhoft, S., Damkilde, L., Krabbenhøft, K. Upper and Lower Bound Calculations of the Bearing Capacity of Strip Footings near Slopes in Cohesionless Soil. In the *International Conference on Structural Engineering, Mechanics and Computation*. 2013. Pp. 2479–2484.
20. Keskin, M.S., Laman, M. Model studies of bearing capacity of strip footing on sand slope. *KSCE Journal of Civil Engineering*. 2013. 17(4). Pp. 699–711.
21. Acharyya, R., Dey, A. Finite element investigation of the bearing capacity of square footings resting on sloping ground. *INAE Letters*. 2017. 2(3). Pp. 97–105.
22. Shukla, R.P., Jakka, R.S. Critical setback distance for a footing resting on slopes. *Acta Geotechnica Slovenica*. 2017. 14(2). Pp. 19–31.
23. Zhou, H., Zheng, G., Yin, X., Jia, R., Yang, X. The bearing capacity and failure mechanism of a vertically loaded strip footing placed on the top of slopes. *Computers and Geotechnics*. 2017. 94. Pp. 12–21.
24. Shukla, R.P., Jakka, R.S. Critical setback distance for a footing resting on slopes under seismic loading. *Geomechanics and Engineering*. 2018. 15(6). Pp. 1193–1205.
25. Mansouri, T., Abbeche, K. Experimental bearing capacity of eccentrically loaded foundation near a slope. *Studia Geotechnica et Mechanica*. 2019. 41(1). Pp. 33–41.
26. Gemberline, M.C. Centrifuge modeling of shallow foundations. *Proc., 11th Int. Conf. on Soil Mech. and foundation Engrg., Balkema, Rotterdam, the Netherlands*. 1988. 2. Pp. 33–36.
27. Shukla, R.P., Jakka, R.S. Discussion of “Experimental and numerical studies of circular footing resting on confined granular subgrade adjacent to slope.” *International Journal of Geomechanics, ASCE*. 2017. 17(2). Pp. 1–3.
28. Van Baars, S. The inclination and shape factors for the bearing capacity of footings. *Soils and Foundations*. 2014. 54(5). Pp. 985–992.
29. Castelli, F., Motta, E. Seismic bearing capacity of shallow foundations. In *Earthquake-Resistant Structures-Design, Assessment and Rehabilitation*. IntechOpen. 2012.
30. Makrodimopoulos, A., Martin, C.M. Upper bound limit analysis using simplex strain elements and second-order cone programming. *International journal for numerical and analytical methods in geomechanics*. 2007. 31(6). Pp. 835–86.
31. Makrodimopoulos, A., Martin, C.M. Lower bound limit analysis of cohesive frictional materials using second-order cone programming. *International Journal of Solids and Structures*. 2006. 44(4). Pp. 604–634.
32. Krabbenhøft, K., Lyamin, A.V., Sloan, S.W. Formulation and solution of some plasticity problems as conic programs. *International Journal of Solids and Structures*. 2007. 44(5). Pp. 1533–1549.
33. Krabbenhøft, K., Lyamin, A.V., Sloan, S.W. Three-dimensional Mohr-Coulomb limit analysis using semidefinite programming. *Communications in Numerical Methods in Engineering*. 2008. 24(11). Pp. 1107–1119.
34. Alencar, A.S., Galindo, R.A., Melentjevic, S. Bearing capacity of foundation on rock mass depending on footing shape and interface roughness. *Geomechanics and Engineering*. 2019. 18(4). Pp. 391–406.
35. Shukla, R.P. Pile groups subjected to abrupt collapse of retaining structure. *Građevinar*. 2018. 70(11). Pp. 953–964.
36. Indian Standard, IS: 2720 (Part IV)-1975. *Methods of test for soils: Part 4 Grain size analysis*. India: Bureau of Indian Standards. 2006.
37. Rostami, V., Ghazavi, M. Analytical solution for calculation of bearing capacity of shallow foundations on geogrid-reinforced sand slope. *Iranian Journal of Science and Technology: Transactions of Civil Engineering*. 2015. 39(C1). Pp. 167–182.

38. Chang, J.C., Liao, J.J., Pan, Y.W. Bearing behavior and failure mechanism of a shallow foundation located on/behind the crest of a poorly cemented artificial sandstone. *International Journal of Rock Mechanics and Mining Sciences*. 2008. 45(8). Pp. 1508–1518.
39. Gamier, J., Canepa, Y., Corte, J.F., Bakir, N.E. Etude de la Portance de Fondations en Bord de Talus. 13th Int. Conf. on Soil Mechanics and Foundation Engineering. 1994. 2. Pp. 705–708.
40. Absi, E. La théorie des équivalences et son application à l'étude des ouvrages d'art. In *Annales de ITBTP*. 1972. 295. Pp. 61–90.
41. Giroud, J.P. et Tran-Vo-Nhiem. Force portante d'une fondation sur une pente. : A.I.T.B.T.P. No. 283–284 juillet-août, Série: théorie et méthodes de calcul. 1971. 142.
42. Mizuno, T., Takumitsu, Y., Kavakami, H. On the bearing capacity of a slope of cohesionless soil. *Soils and Foundations*. 1060. 1(20). Pp. 30–37.
43. Chen, W.F., Davidson, H.L. Bearing capacity determination by limit analysis. *Journal of the Soil Mechanics and Foundations Division*. 1973. 99(6). Pp. 433–449.
44. Tatsuoka, F., Huang, C.C., Morimoto, T., Okahara, M. Discussion of stress characteristics for shallow footing in cohesionless slopes. *Canadian Geotech. J.* 1989b. 26. Pp. 748–755.
45. Lebegue, Y. Essais de fondations superficielles sur talus. 8th International Conference on Soil Mechanics and Foundation Engineering, Moscow. 1973. 4(3). 313 p.

Contact:

Rajesh Prasad Shukla, rpshukla.2013@iitkalumni.org

Ravi S. Jakka, rsjakka@iitr.ac.in

© Shukla, R.P., Jakka, R.S., 2021